UNRESTRICTED

Daniel Berg 12-30-74
Director Date

Daniel Berg, Manager
Energy Systems Division

APPROVED: Daniel Berg

Daniel Berg, Manager
Energy Systems Division

REK MeL

WORK PERFORMED UNDER CONTRACT AT(11-1)3045
U.S. ATOMIC ENERGY COMMISSION

MEASUREMENTS OF VELOCITIES DOWNSTREAM OF BLOCKED SUBCHANNELS IN A MODEL REACTOR ROD BUNDLE

B. J. Vegter and R. M. Roidt
Heat Transfer and Fluid Dynamics

M. J. Pechersky and R. A. Markley
Advanced Reactors Division

Research Report 74-8E9-RODS-R1

December 30, 1974

WESTINGHOUSE RESEARCH LABORATORIES Pittsburgh, Pennsylvania 15235

Research Report 74-8E9-RODS-R1
Proprietary Class: Unrestricted

December 30, 1974

MEASUREMENTS OF VELOCITIES DOWNSTREAM OF BLOCKED SUBCHANNELS IN A MODEL REACTOR ROD BUNDLE

B. J. Vegter and R. M. Roidt
Heat Transfer & Fluid Dynamics

M. J. Pechersky and R. A. Markley
Advanced Reactors Division

ABSTRACT

Two blockage configurations were installed on the upstream end of a hexagonal grid in an 11:1 scale 39 rod bundle air model of a liquid metal fast breeder reactor. Velocities were measured in subchannels behind and adjoining the blockages. The region of separated flow was found to be five times a characteristic height of the blockages, consistent with other experimental results. The effect of the grids on the length of separated flow was minimal. Flow rates in subchannels centered downstream of the blockages recovered to 90% of the upstream flow rates in the 28 rod diameter length between grids.

TABLE OF CONTENTS

Research Report 74-8E9-RODS-R1
Proprietary Class: Unrestricted

December 30, 1974

MEASUREMENTS OF VELOCITIES DOWNSTREAM OF BLOCKED SUBCHANNELS IN A MODEL REACTOR ROD BUNDLE

B. J. Vegter and R. M. Roidt
Heat Transfer & Fluid Dynamics

M. J. Pechersky and R. A. Markley
Advanced Reactors Division

I. INTRODUCTION

In a liquid metal fast breeder reactor (LMFBR) it is important to know the length of the region of separated flow behind a blockage in order to evaluate the likelihood that the "hot spot" behind the obstruction will result in fuel cladding melting and eventually shutdown of the reactor. One proposed design of a LMFBR employs hexagonal grids for supporting fuel rods. In such a design the most likely blockage would occur from the collection of debris suspended in the fluid at the upstream end of a hexagonal grid. This investigation examined for two different configurations of blockages the downstream recovery of subchannel flow rate and the distance over which the flow remained separated.

II. RESULTS AND CONCLUSIONS

The length of the region of separated or reversed flow behind a completely blocked single subchannel was observed to be 5.4 times the characteristic obstruction height, i.e., the distance from the subchannel centroid to the clearance gap. Behind a blockage consisting of a central channel and its three adjoining subchannels this length was found to be 4.7 times the characteristic obstruction height, in this case the distance between the blockage centroid and the surface of the opposite rod in the adjoining subchannel. These results agree very well with previous experimental results using similar blockage geometries. The effect of the presence of the grid behind the blockages was minimal. The flow rate in the subchannel centered behind the blockages recovered to 90% of its upstream value in the 28 rod diameter length between grids.

III. EXPERIMENTAL APPARATUS AND PROCEDURES

The experimental apparatus with the exception of the blockages has previously been described in Reference 1. Thirty nine 2.5 inch diameter rods arranged in a hexagonal array were enclosed by an aluminum duct (Figure 1) forming part of an 11:1 scale air model of a 217 pin fuel assembly (Figure 2). The rods were supported by three honeycomb grids (Figures 3 and 4). To the upstream end of the middle grid were attached two blockages constructed of 1/4 inch thick Plexiglas. Configuration A blocked off completely one subchannel, configuration B closed off in addition the three adjacent subchannels (Figures 1 and 5).

Three rods, instrumented with 0.0625 inch diameter pitot static tubes facing upstream, were used to record velocities at axial locations ranging from 22 inches upstream to 65 inches downstream of the blockage. The cross-sectional position of a reading was determined as follows: the subchannel is designated according to Figure 6 and the location within the subchannel is found according to Figure 7.

For each configuration two different experiments were made, one to determine the region of separated flow by describing the locus of zero velocity points downstream of the obstruction, henceforth to be called "the zero velocity experiment". The other experiment determined the recovery of flow rates downstream of the blockage, henceforth to be called "the subchannel flow rate test".

For the zero velocity experiment, readings were taken at the positions indicated in Figure 7 in subchannel 2,3 of Figure 6. Fewer data points were used for configuration A as the locus of zero velocity points was found to occur within the grid where the motion of the pitot tube was restricted. For the flow rate recovery experiment five readings (Figure 7) were taken in each subchannel and used to estimate the average subchannel velocity. Readings were taken in subchannels 2,2; 2,3; 2,4; and 3,6 for both blockage configurations and in addition subchannels 1,4; 1,5; and 3,1 for configuration B (Figure 6).

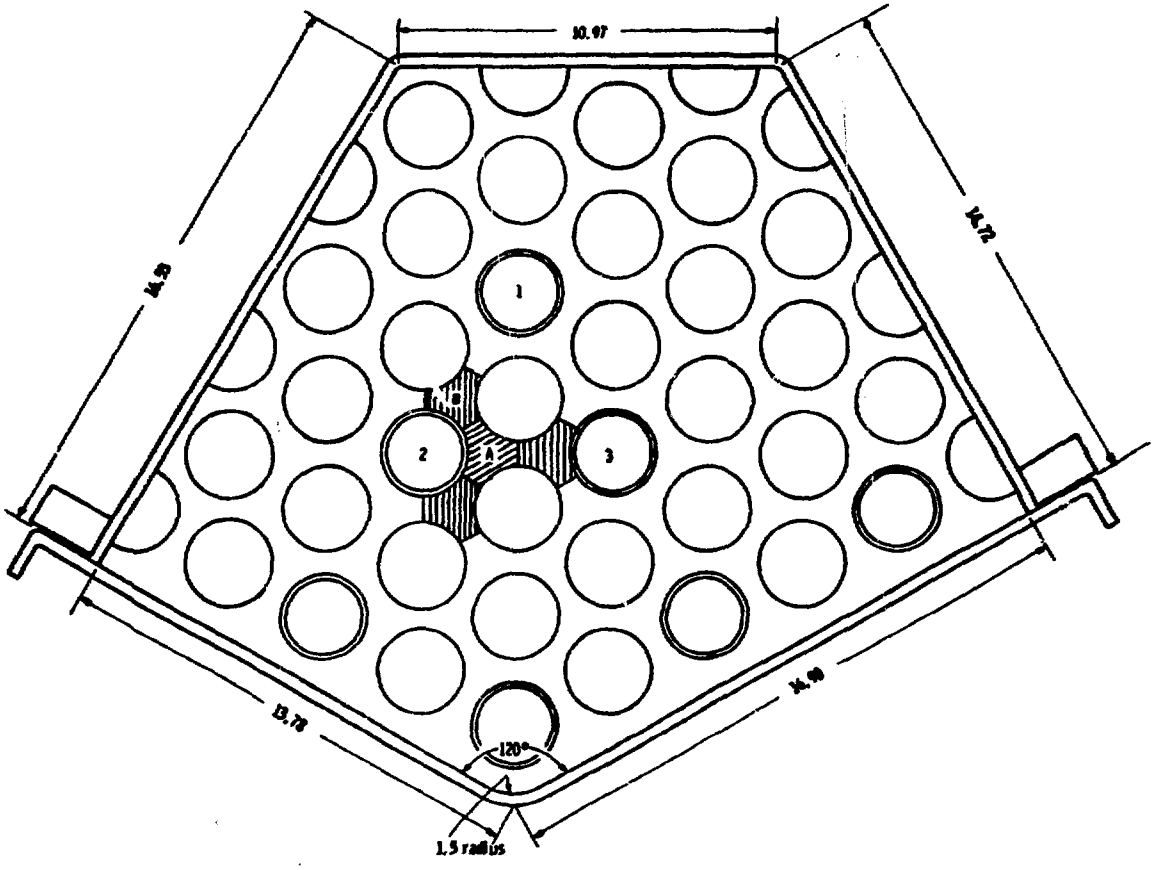

Figure 1. Cross-Section of Test Section (Dimensions In Inches) With Location of Blockages

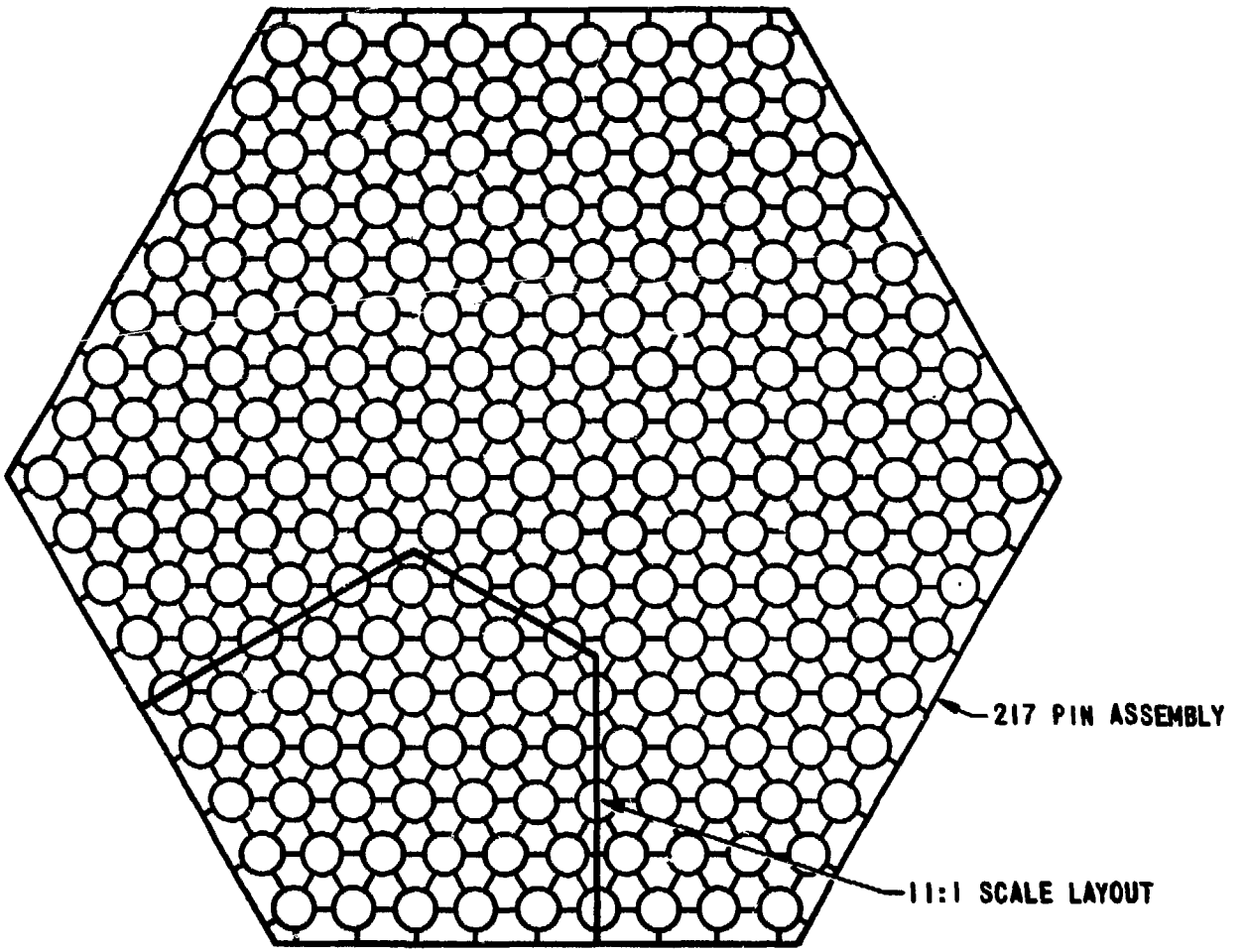

Figure 2. 217 Pin Fuel Assembly With 11:1 Scale Model Cross Section Super-Imposed

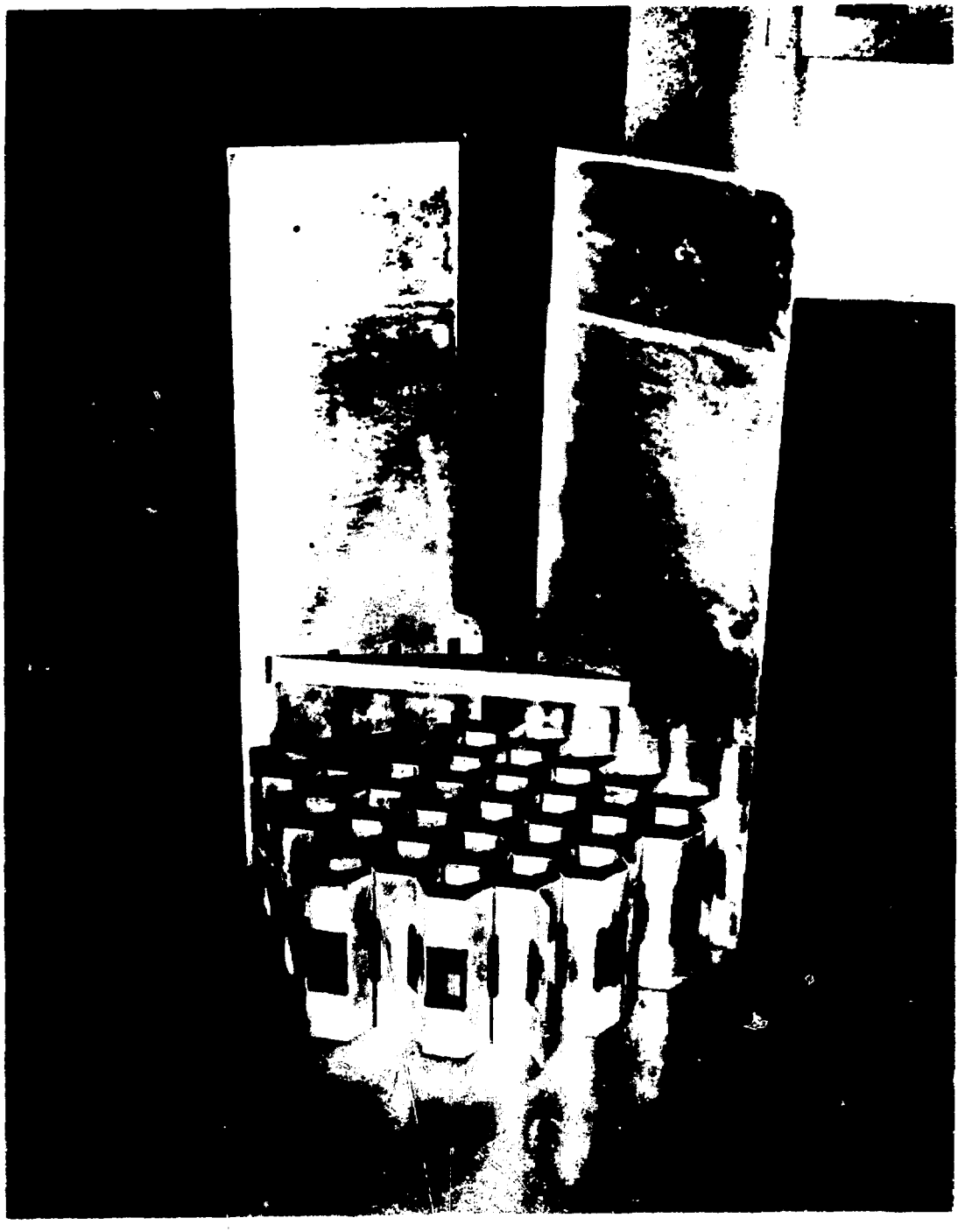

Figure 3. 11 to 1 Scale Test Grid

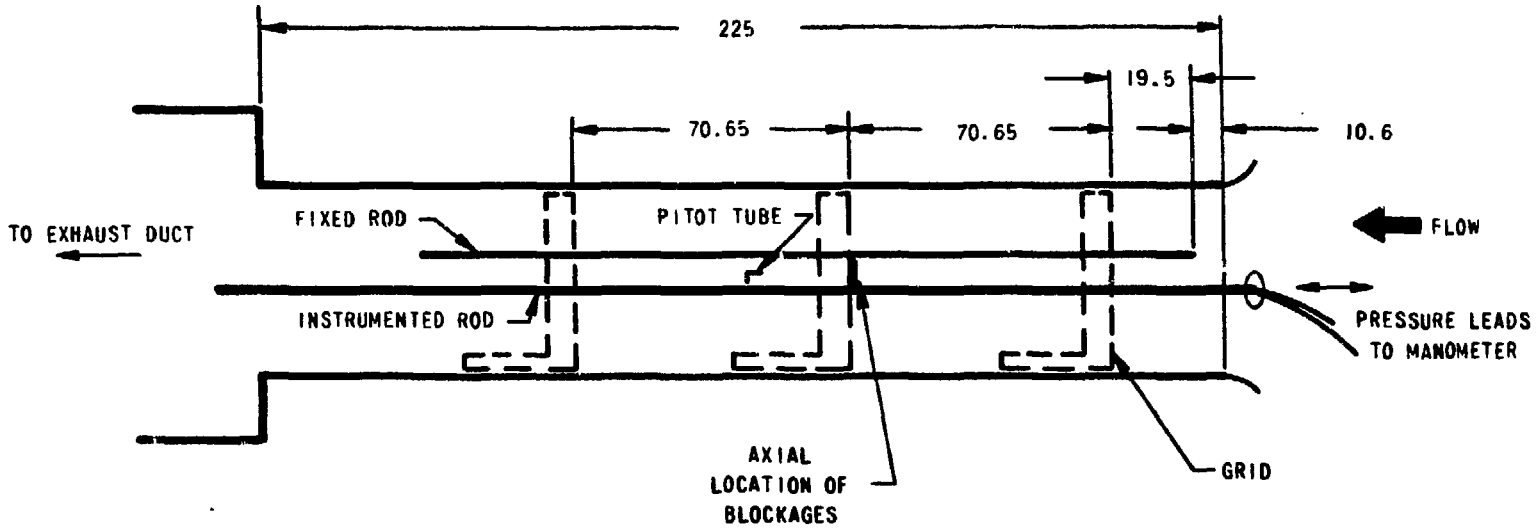

Figure 4. Schematic of 11:1 Scale Rod Bundle Air Flow Test (Gridded) (Dimensions in Inches)

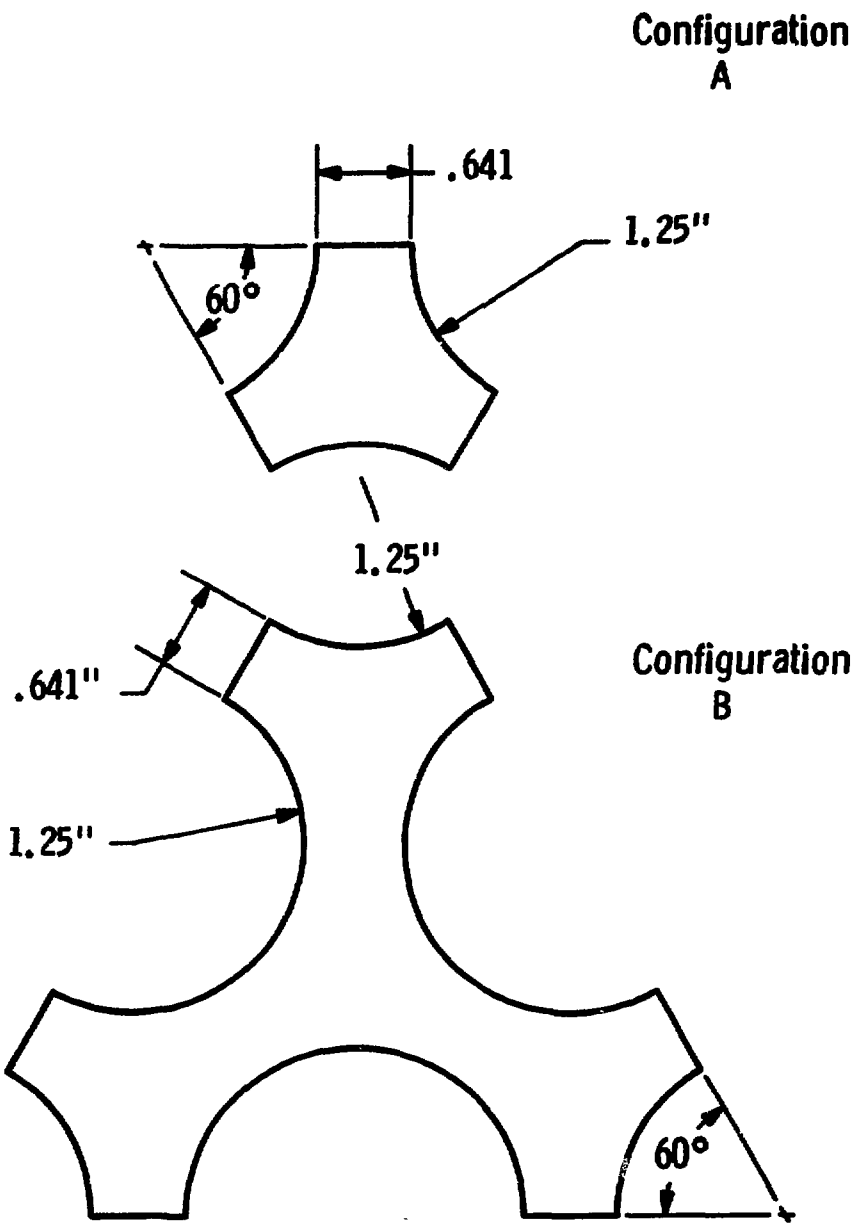

Fig. 5—Blockage Configurations

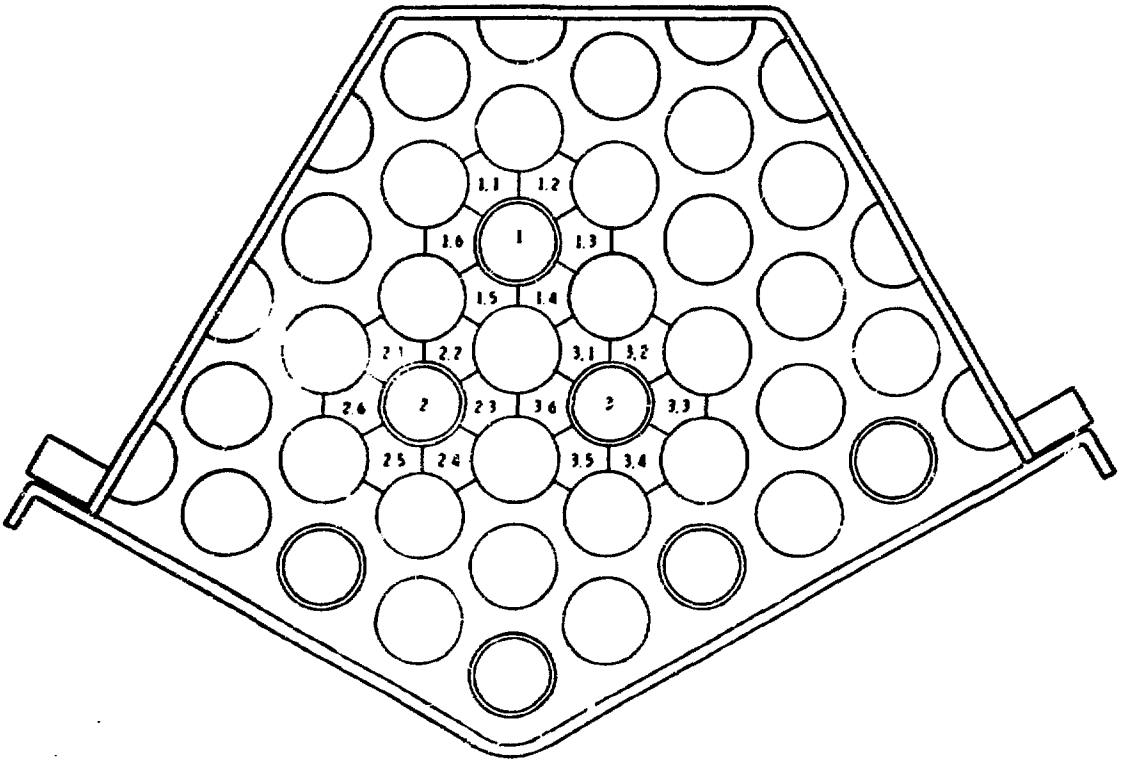

Figure 6. Numbering of Experimental Subchannels

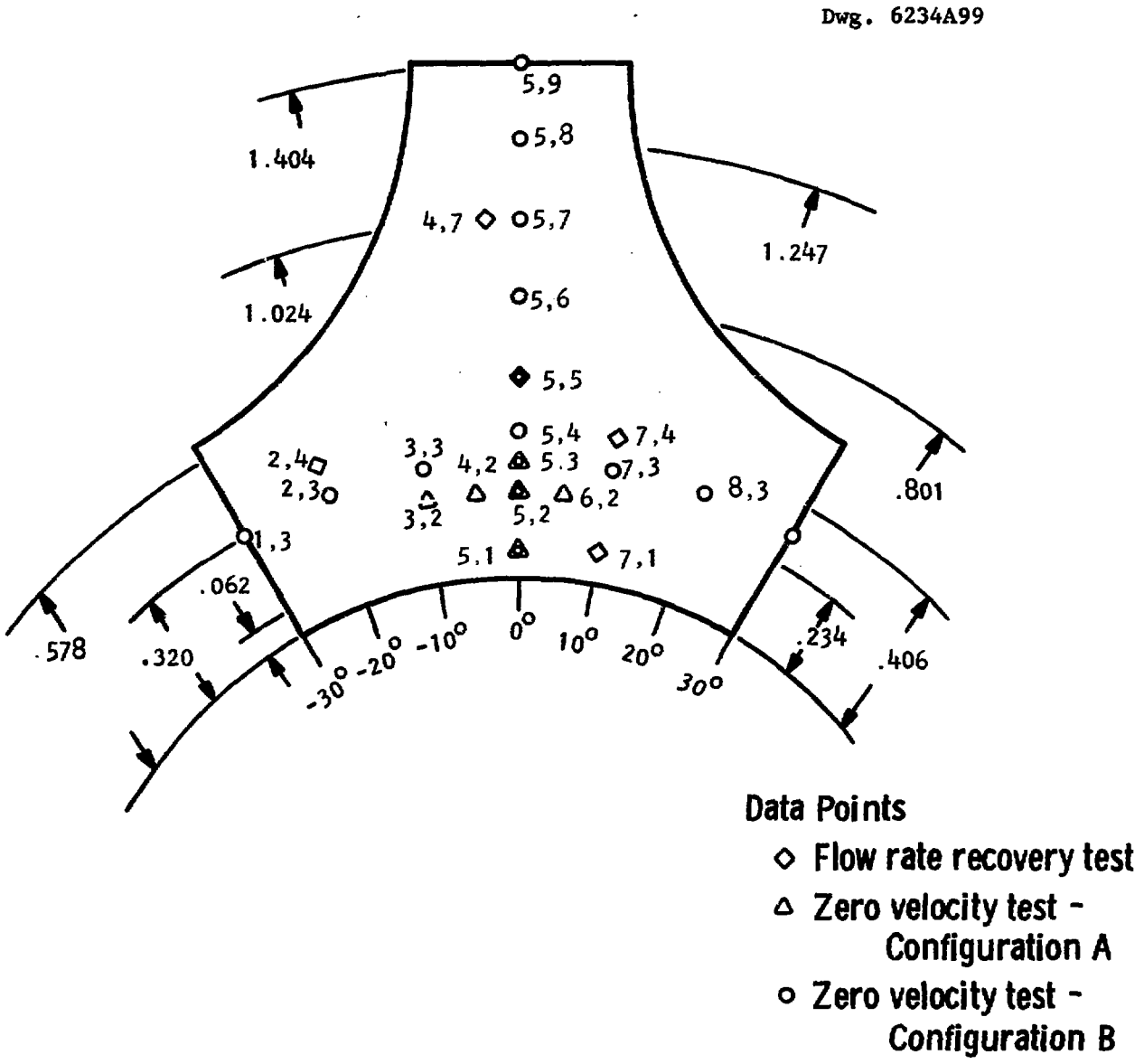

Fig. 7—Inboard subchannel with location of data points (Dimensions in inches)

For the pitot tube used, there was a separation distance of 0.25 inches between static and stagnation taps. Pressure differences were recorded using an inclined manometer with 0.834 specific gravity oil. The calculated velocities were normalized with respect to the mean velocity through the rod bundle as determined by measuring the flow rate through the exhaust duct. For these experiments the mean velocity was 78.07 ft/sec and the rod bundle Reynolds number was 71,100.

IV. EXPERIMENTAL RESULTS

A. Discussion

Use of a pitot static probe restricted readings to the region outside of the recirculating flow. Therefore, velocities downstream of this region were measured and the axial velocity profile extrapolated upstream to find a locus of zero velocity points. The zero velocity points can be used instead of the locus of points where the stream function is zero, the usual definition for the extent of separated flow, since for symmetric flow around a blockage the two loci coincide.

In the region downstream of recirculation, the flow is not purely axial and therefore is not aligned with the pitot static tube. Error in stagnation and static pressure increase rapidly for angles of attack greater than 5^{o}. However, the modified Prandtl type pitot static tube used in this experiment is designed so that errors in stagnation and static pressure compensate each other, yielding velocity readings accurate to 2% for angles of attack of up to 30 degrees.

Because the static pressure tap is 0.25 inches downstream from the stagnation pressure tap instead of being coincident, an error arises in determining the location of the locus of zero velocity points. If there existed no axial gradient in static pressure, no correction would be required. However, due to the observed axial variations in static

and stagnation pressure, the uncertainty in the location of a zero velocity point due to separation of taps is estimated to be ± 0.4 inches. This uncertainty was determined by comparing the axial location where the stagnation pressure equaled the static pressure versus the axial location where the stagnation pressure equaled the static pressure displaced to the tip of the pitot static probe.

B. Small Blockage Results (Configuration A)

1. Zero Velocity Experiment

Table 1 of Appendix A lists the normalized velocity data for the zero velocity experiment using the single subchannel blockage. Figures 8 and 9 show the velocities for various locations downstream from the blockage, where the pitot static probe was located .234 inches radially from the surface of rod 2. From Figure 9 using the curve for point 3,2; it can be seen that the zero velocity point occurs 4.94 inches downstream from the rear of the blockage. This zero velocity point occurs inside the grid and is displaced 10^{o} counterclockwise from the blockage center. The reason for the transverse displacement of the zero velocity point from the blockage centroid and for the asymmetry of the velocity profile in Figure 8 is the asymmetric construction of the hexagonal grid. At 4.1 inches downstream from the rear of the blockage there is a support dimple centered at -30^{o}. This dimple acts as an additional blockage and shifts the zero velocity point counterclockwise.

2. Flow Rate Recovery Experiment

The recovery of flow rate downstream of blockage configuration A is displayed in Figures 10 through 13, and the measured velocities are listed in Table 2 of Appendix A. Figure 10 shows that at 28 rod diameters downstream from the blockage the flow rate in the subchannel behind the blockage is 90% of the value 9 rod diameters upstream from

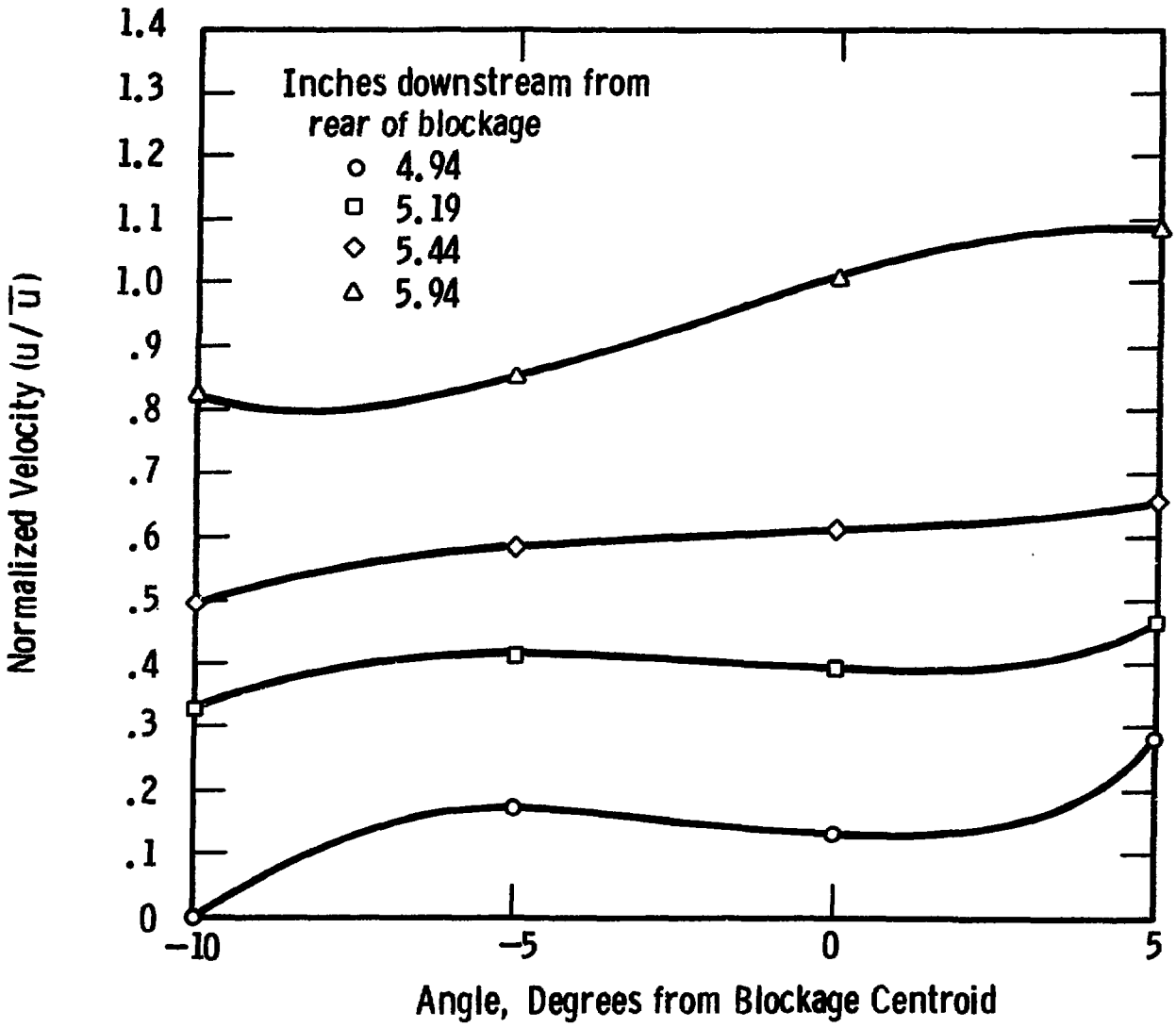

Fig. 8—Transverse velocity profile downstream of small blockage-configuration A

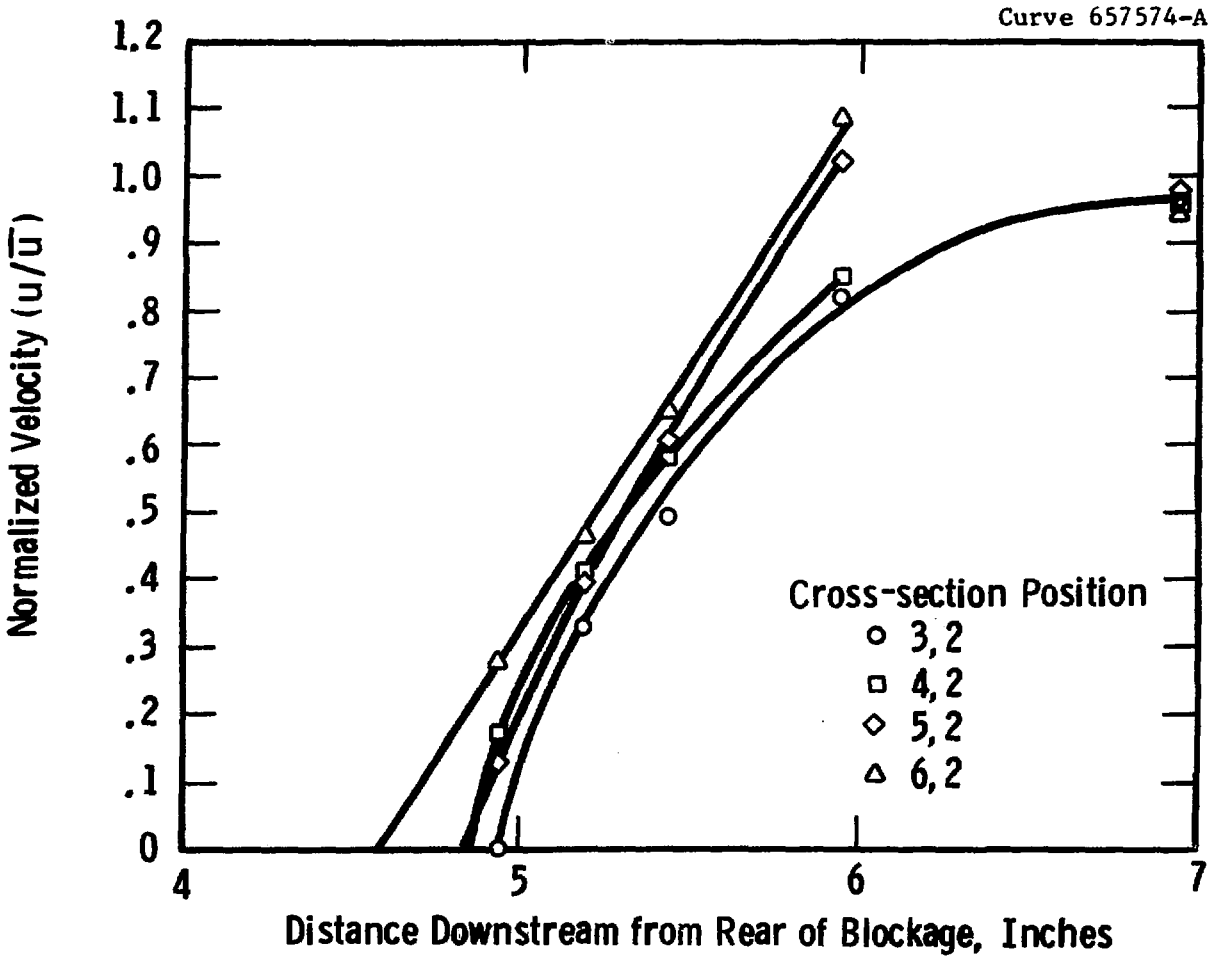

Fig. 9—Location of zero velocity points for small blockage - configuration A

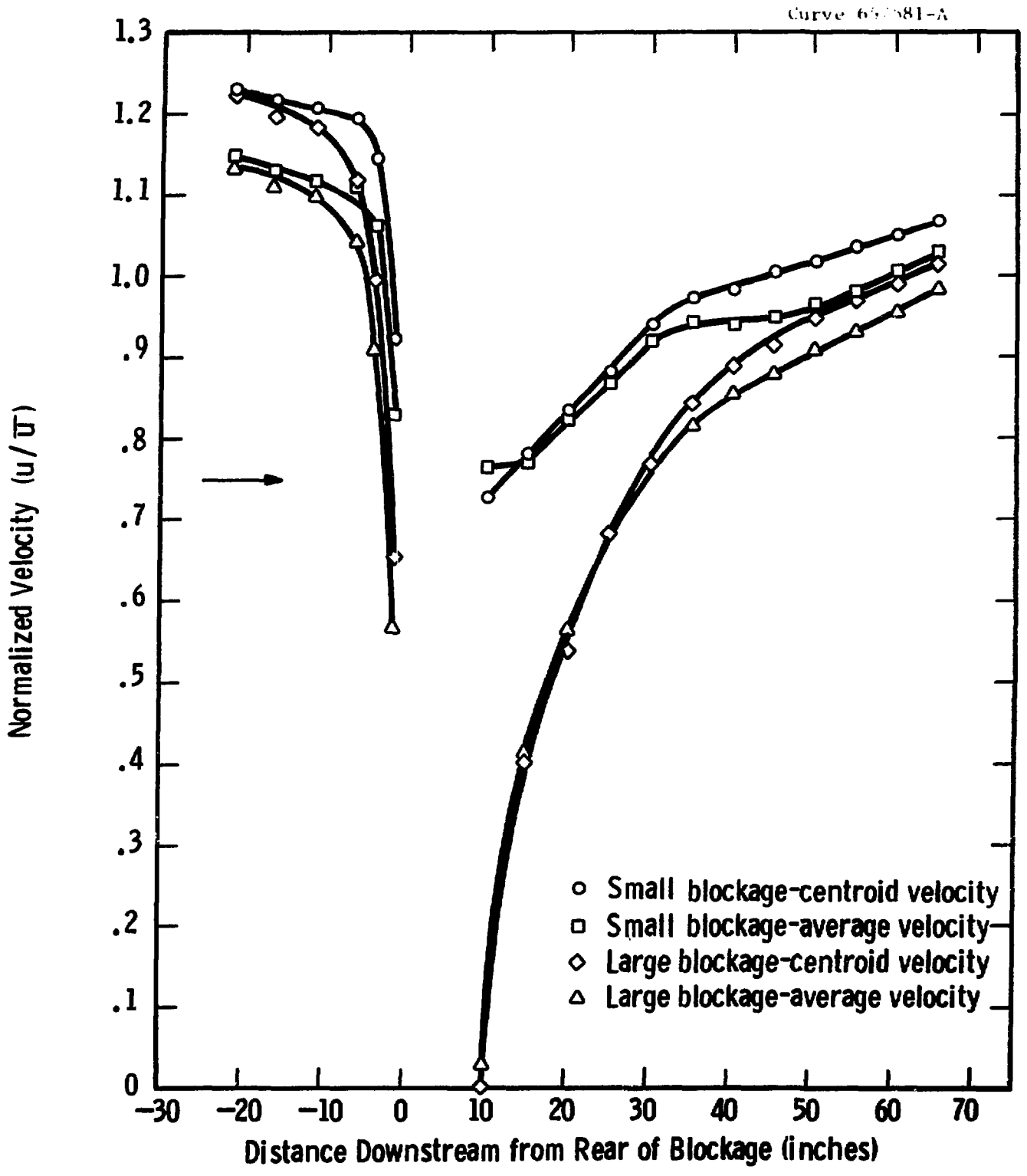

Fig. 10—Axial velocity distribution for subchannel 2,3

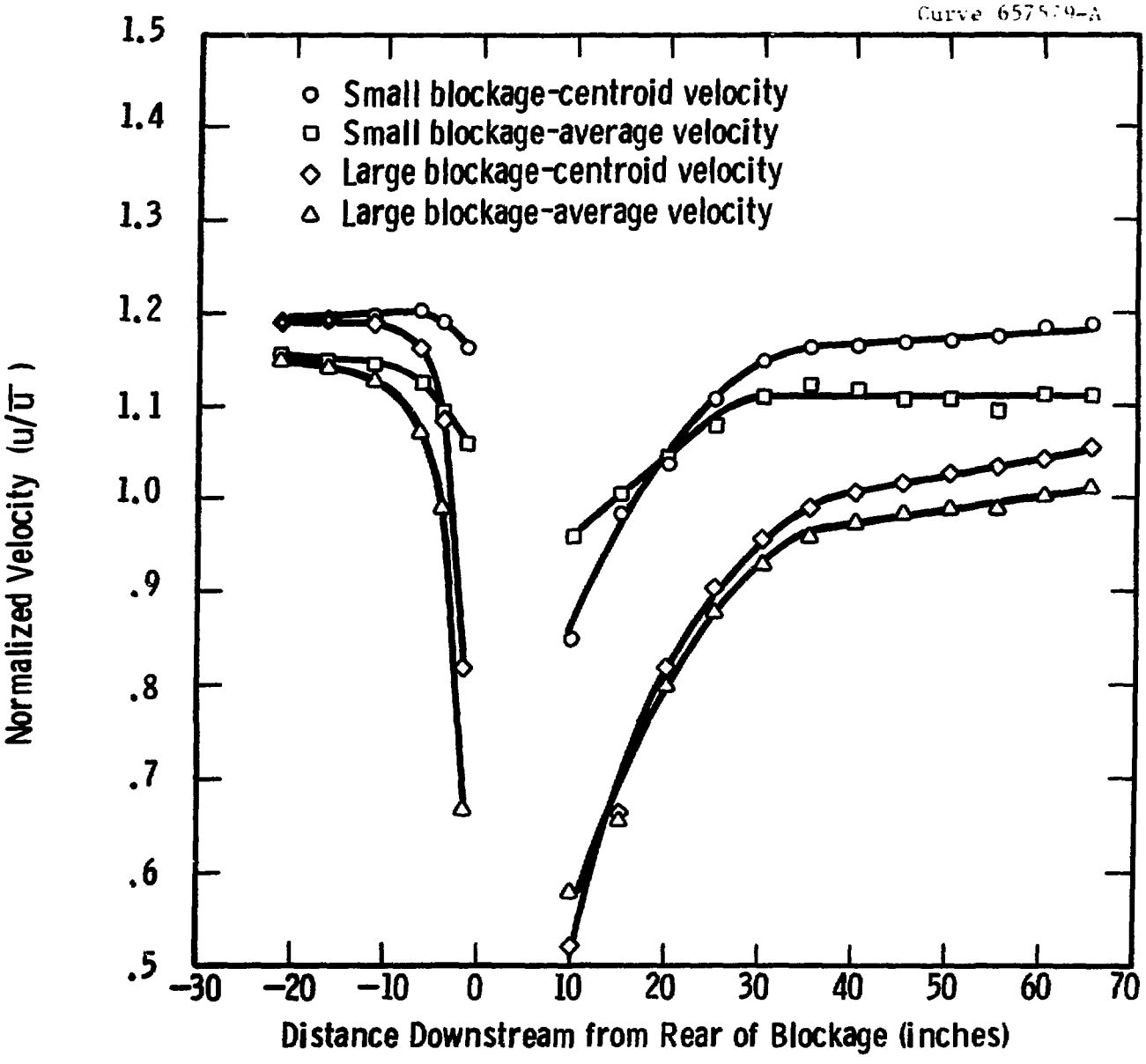

Fig. 11—Axial velocity distribution for subchannel 2, 2

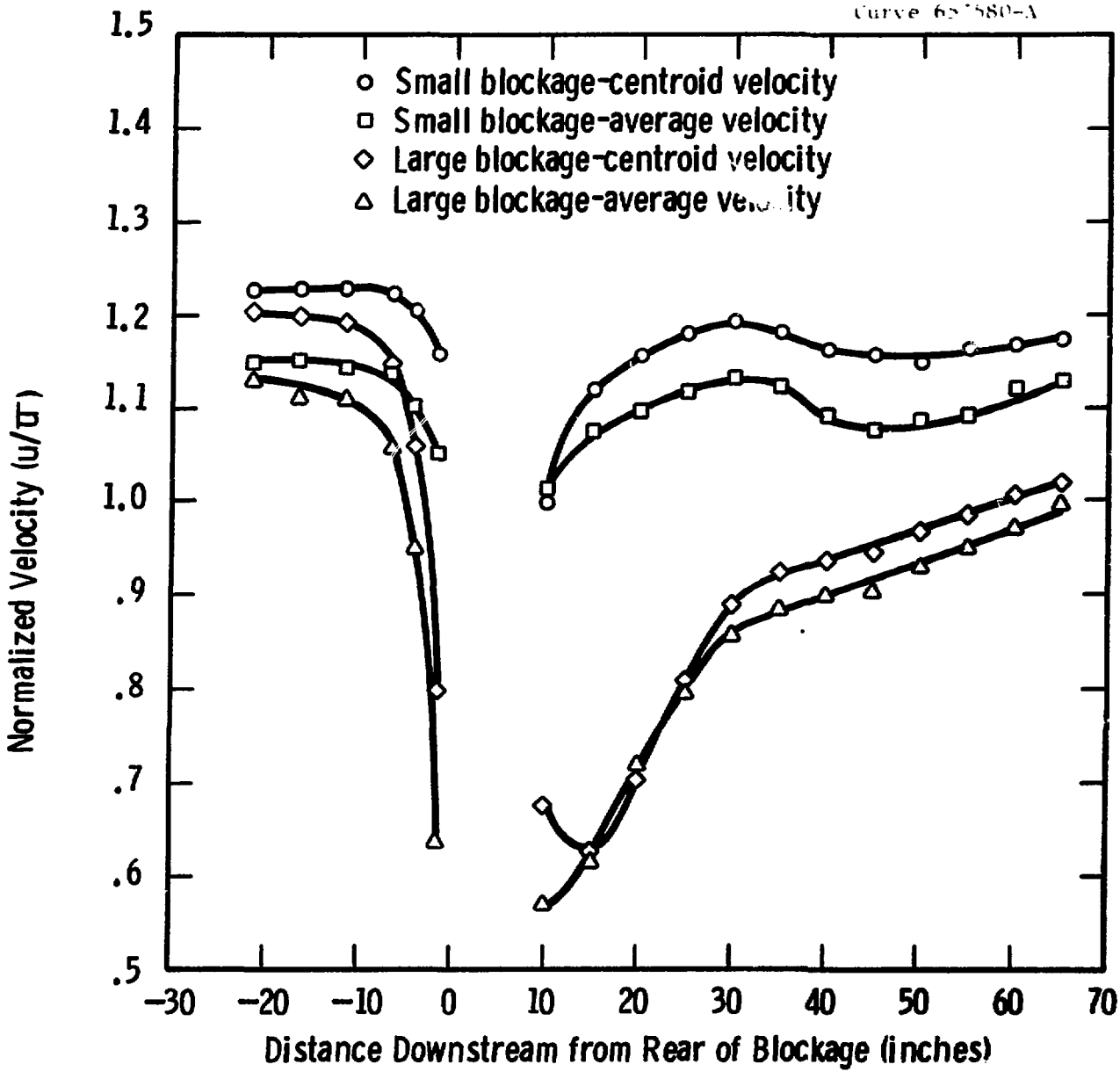

Fig. 12—Axial velocity distribution for subchannel 2,4

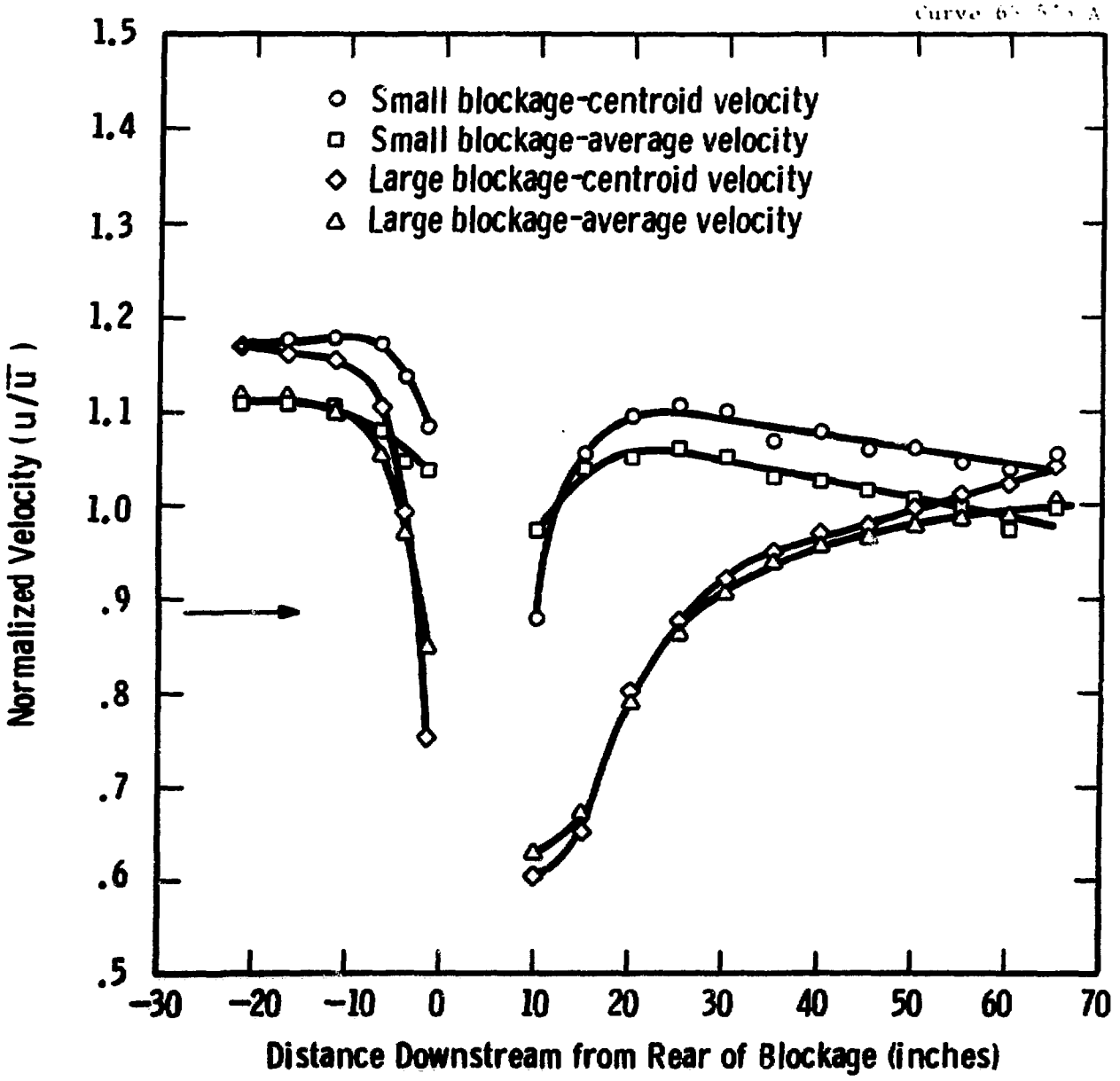

Fig. 13—Axial velocity distribution for subchannel 3, 6

the blockage. Figures 11 through 13 show that the subchannel flow rates of the adjoining subchannels are also affected by the blockage.

C. Large Blockage Results (Configuration B)

1. Zero Velocity Experiment

Table 3 of Appendix A tabulates the results, displayed in Figures 14 and 15 for the zero velocity experiment for the large blockage of four subchannels. From Figure 15 the curve for position 5,3 shows that the zero velocity point occurs 11.28 inches downstream from the rear of the blockage or just over three inches from the rear of the grid. Figure 14 shows that the velocity profile is symmetric with respect to the blockage centroid and that the reduced centroid velocities extend over 20 inches downstream of the blockage.

2. Flow Rate Recovery Experiment

The recovery of flow rate downstream of blockage configuration B is shown in Figures 10 through 13 and Figures 16 through 18, with the measured velocities listed in Table 4. As with configuration A, the subchannel flow rate in the channel centered behind the blockage recovers to 90% of its upstream value at 28 rod diameters downstream.

V. DISCUSSION

The most important result of this experiment is the calculation of the length (L) of the region of separated flow, where L is measured from the rear of the blockage. For configuration A the length of this region was observed to be 4.94 inches, for configuration B - 11.28 inches. In order to compare these results with other blockage studies these lengths are normalized with respect to a characteristic blockage height (h), usually the distance from the centroid to the edge of the blockage. We feel that if the values of L/h obtained experimentally are similar to those of simpler geometries, for a first approximation the

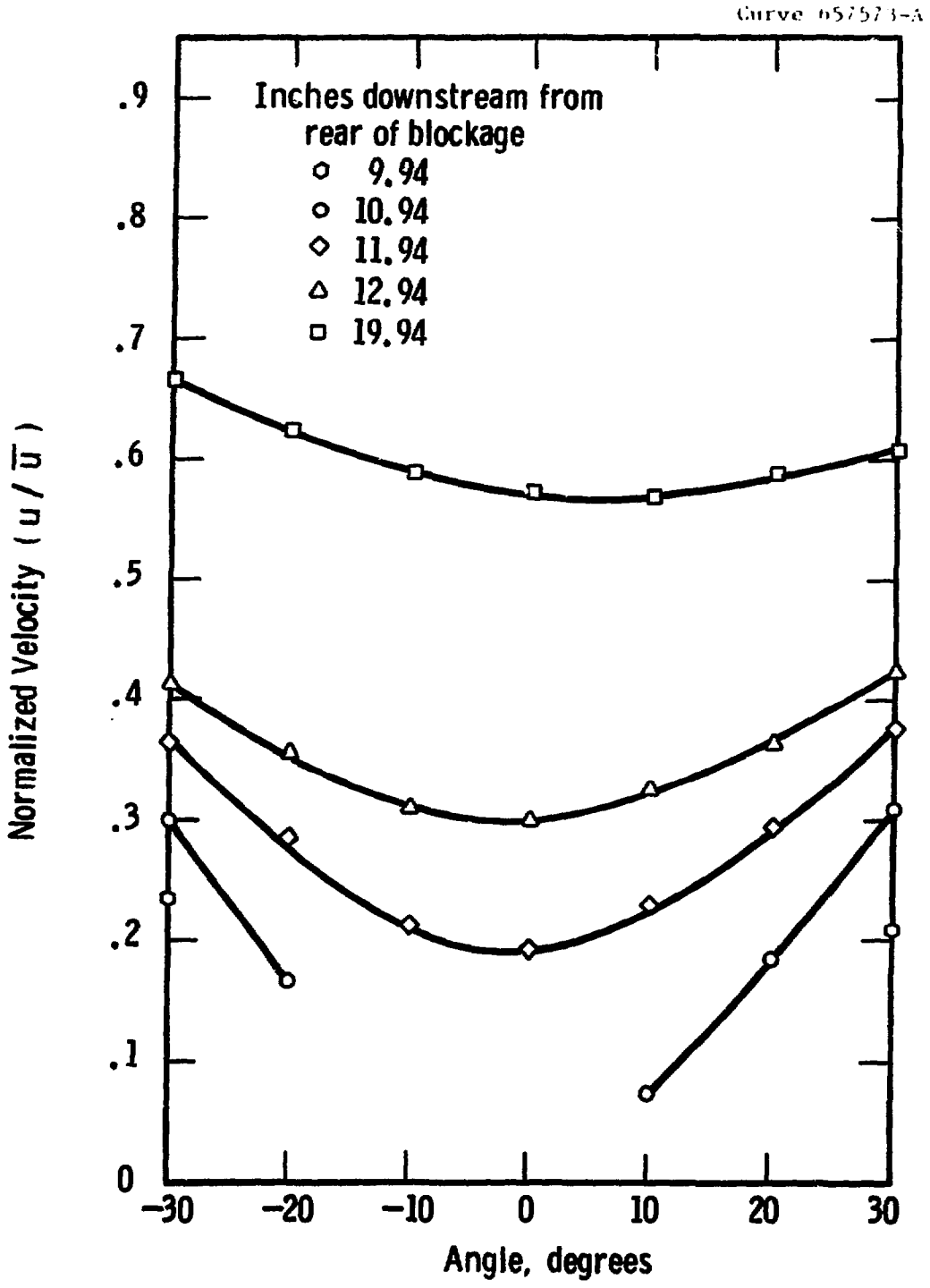

Fig. 14—Transverse velocity profile downstream of large blockage-configuration B

Curve 657571-A

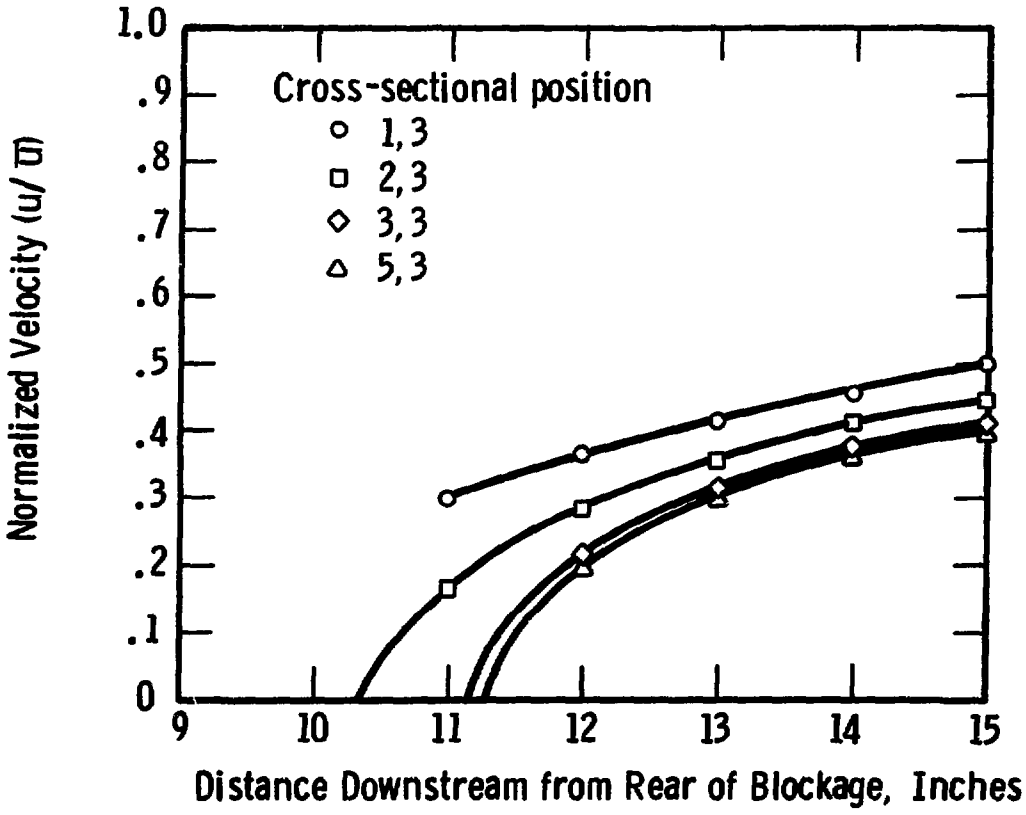

Fig. 15—Location of zero velocity points for large blockage-configuration B

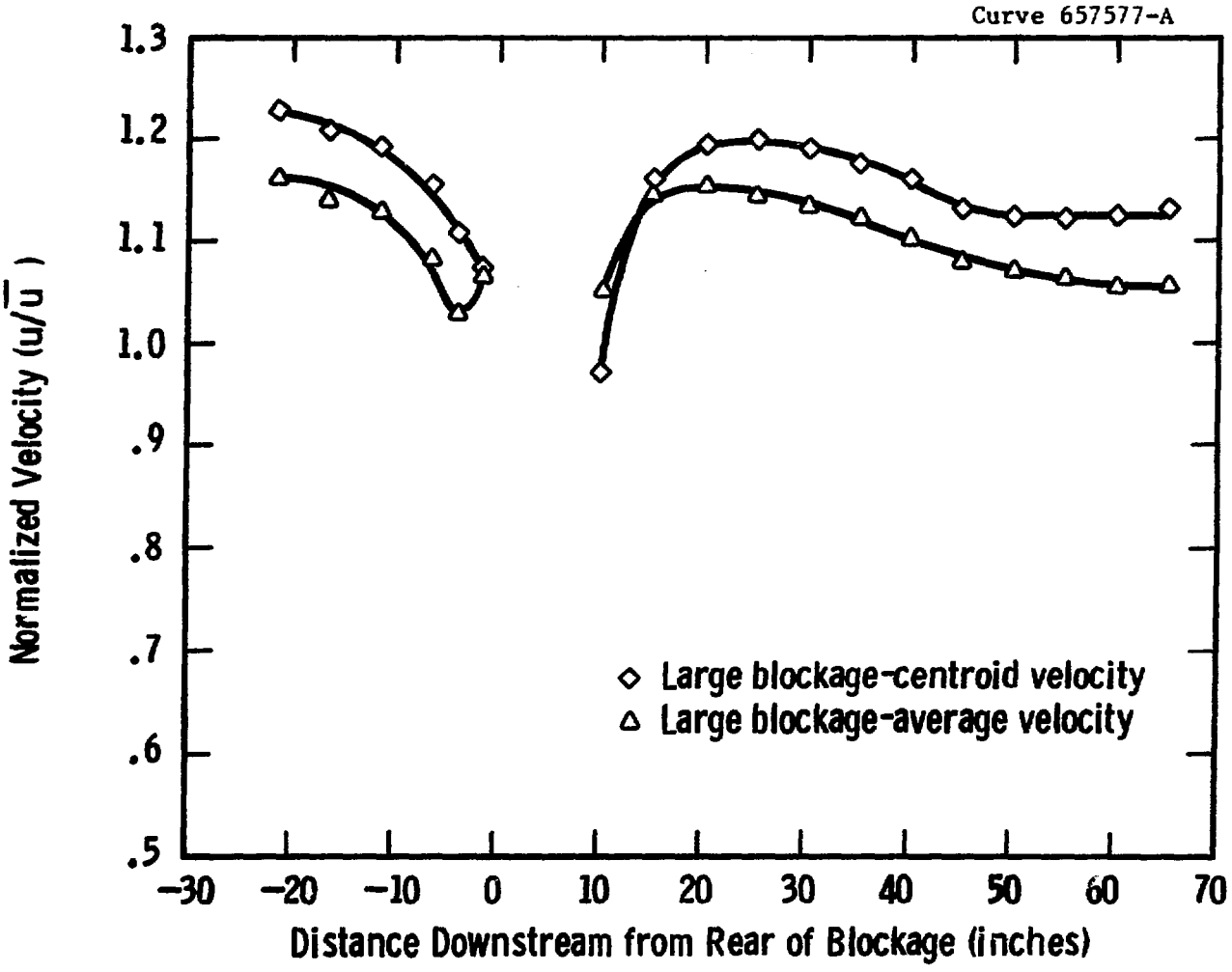

Fig. 16—Axial velocity distribution for subchannel 3, 1

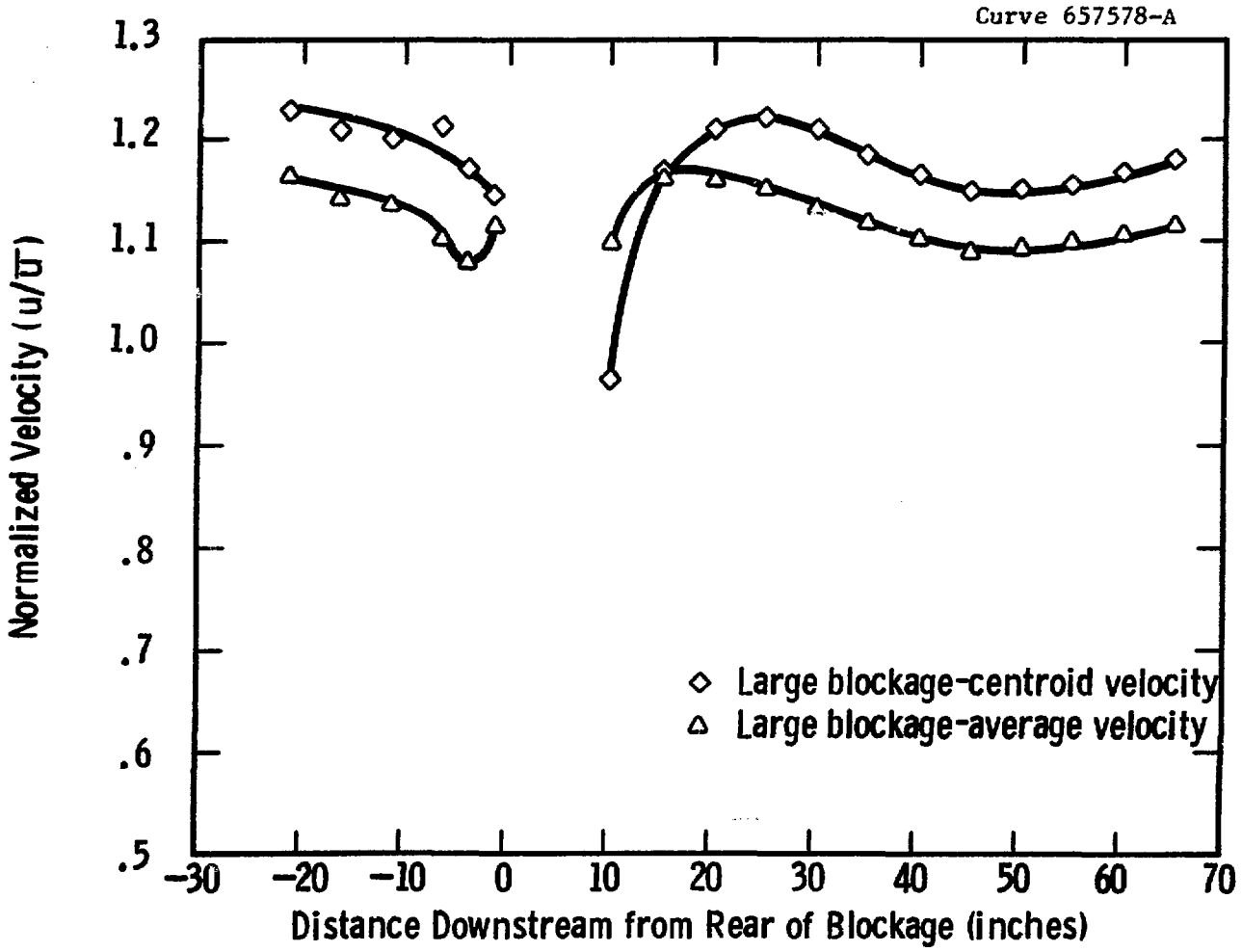

Fig. 17—Axial velocity distribution for subchannel 1, 5

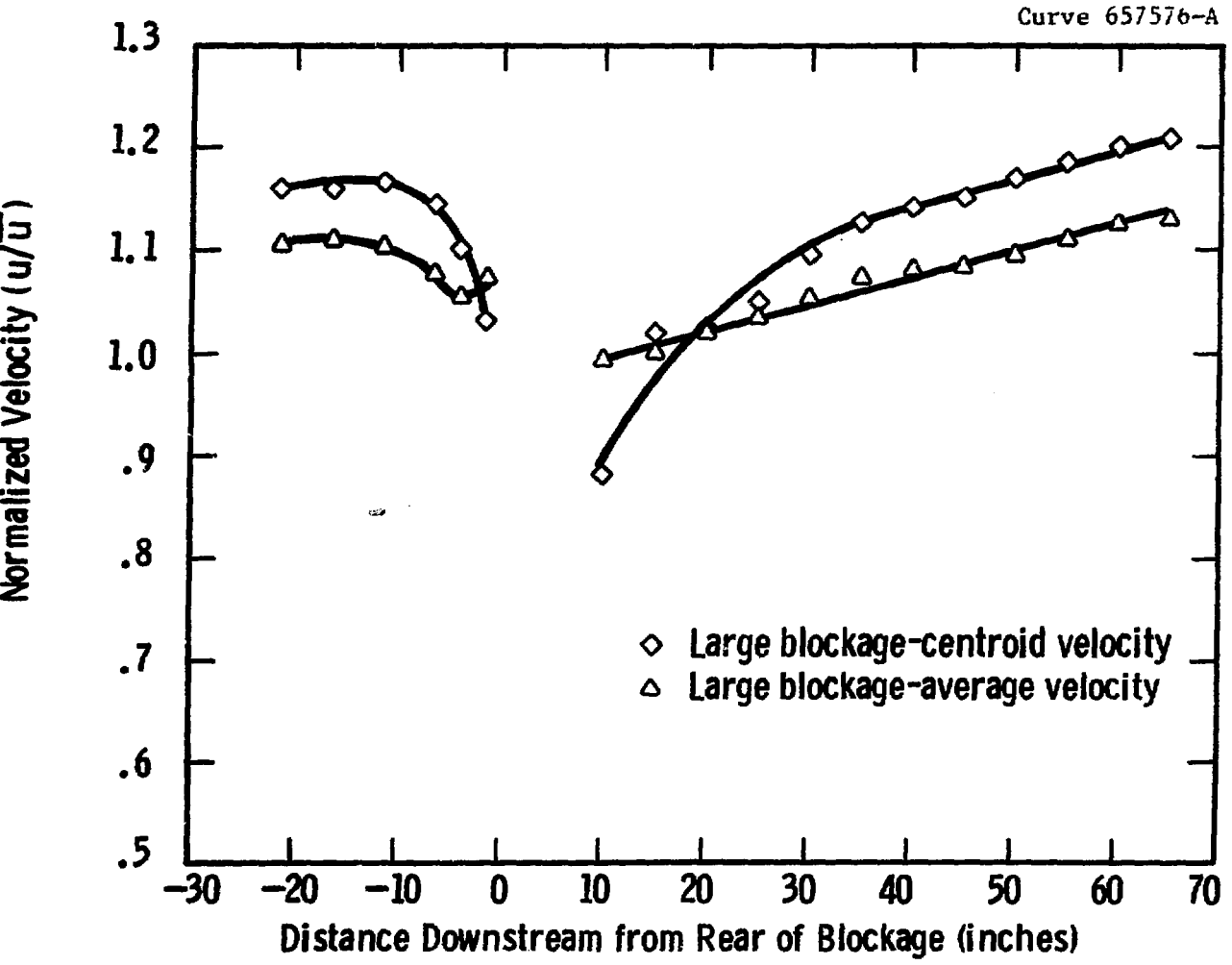

Fig. 18—Axial velocity distribution for subchannel 1, 4

simpler geometry can be used for determining recirculation velocities and heat transfer coefficients.

Reference 2 contains L/h values for various geometries where the pertinent values are listed below:

(a) Two dimensional flow over a step of depth, h, between two large flat plates — $L/h \tilde{\sim} 6\text{-}8$

(b) Two dimensional flow over a sharp edged rectangular obstruction in a free stream — $L/h = 4.6$

(c) Three dimensional flow over a circular sharp edged disk held normal to the flow — $L/h = 5.2$

Experimental work was also performed by Tang and Roidt[3] who examined two blockages, the first similar to configuration A, the second a blockage of the six subchannels surrounding a single rod. They employed a seven rod bundle duct and used thick tapered blockages with no grids behind the blockage. Meausring an L' from the upstream end of their blockages they obtained for L'/h 6.2 and 7.2 for the smaller and larger blockages respectively.

In the current experiment for configuration A, L/h was found to be 5.4 where h is measured from the subchannel centroid to the clearance gap (Figure 19-length a). This agrees very well with Tang and Roidt's value of 6.2 for a similar blockage and with the results observed for the simpler geometries listed above.

It is important to note that the entire region of separated flow for configuration A occurs inside the hexagonal grid. It appears that the restriction on crossflow posed by the walls of the grid is counterbalanced by the mixing provided by interference with dimples and flow through slots so that the hexagonal grid has no significant effect on the length of the separated flow region.

For configuration B, three different blockage heights could be used as indicated in Figure 19. Using length b we obtain L/h = 4.7

Dwg. 6234A91

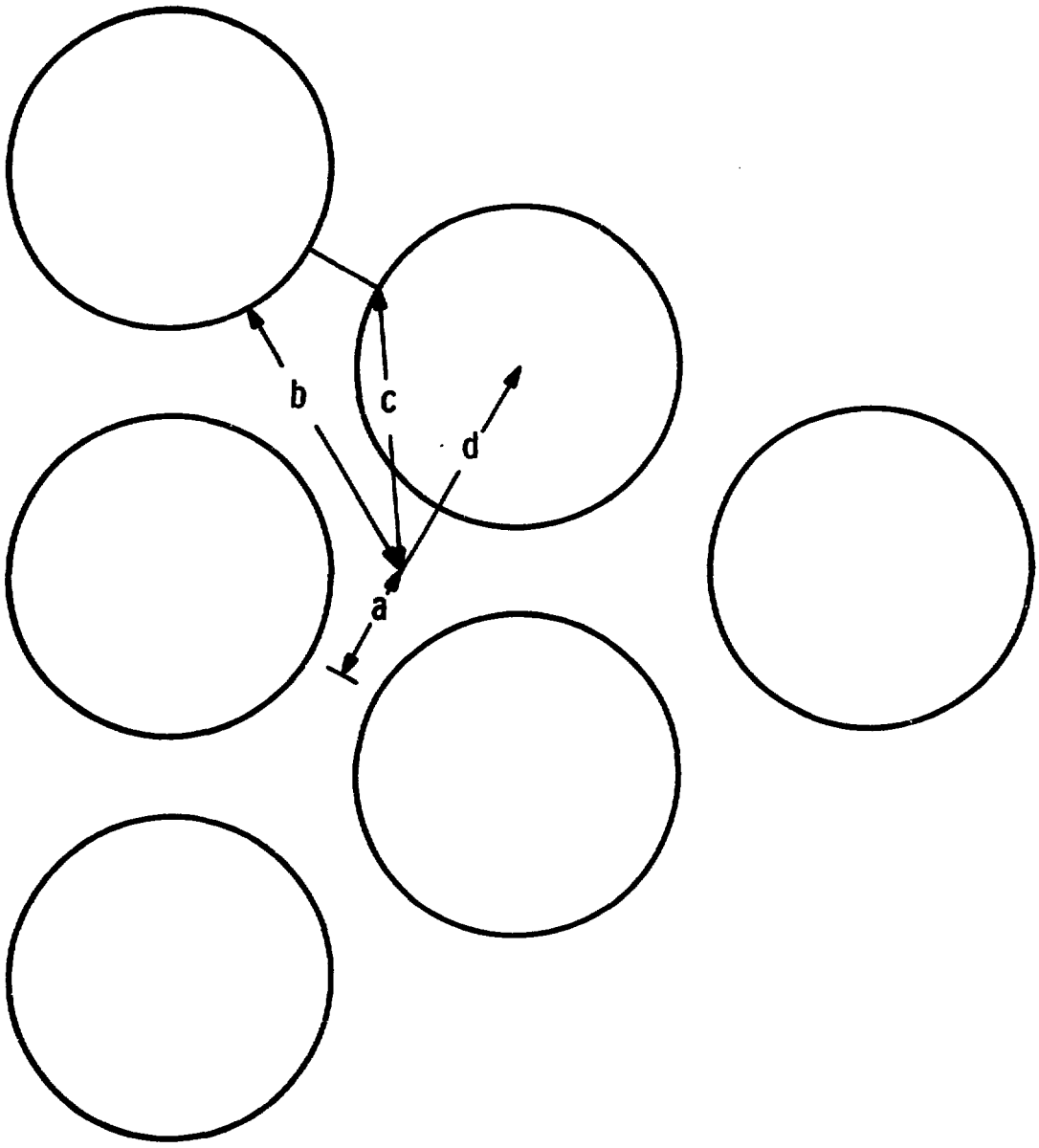

Fig. 19—Characteristic blockage heights

which is consistent with the results for simpler geometries. For configuration B about 75% of the separated flow region occurs within the grid. As with configuration A, the presence of the hexagonal grid does not appear to affect the length of the separated flow region. Although the grid is asymmetric, the velocity profile behind the grid is symmetric as shown in Figure 17.

ACKNOWLEDGMENT

The authors would like to acknowledge the work of E.L. Thomas of Westinghouse Research Laboratories, Heat Transfer and Fluid Dynamics, in performing the experiments. The authors are indebted to P.S. Sherba of Westinghouse Advanced Reactors Division, Thermal and Hydaulics Group, for his many helpful suggestions.

REFERENCES

1. Pechersky, M.J., R. M. Roidt, B. J. Vegter, R. A. Markley, "11:1 Scale Rod Bundle Flow Tests - Parts 1 through 7", U.S. Atomic Energy Commission Report WARD-)X-3045-6, February 1974.

2. Bishop, A. A., J. Graham, J. A. Zoubek, "Hydrodynamic Characteristics of a Wake Behind a Fuel Assembly Local Flow Blockage", Trans. Am. Nuc. Soc., Winter 1971, p. 748.

3. Tang, Y.S., R. M. Roidt, J. A. Zoubek, "Velocity Measurements and Heat Transfer in the Wake of a Flow Blockage in a LMFBR", AIChE Paper No. 34, AIChE-ASME Heat Transfer Conf., Denver, Colorado, August 1972.

PERMANENT RECORD BOOK ENTRIES
Book No. 206219 ... Pgs. 14-15, 42-63

APPENDIX A

EXPERIMENTAL RESULTS

Dwg. n2146A9.

TABLE 1

NORMALIZED VELOCITY MEASUREMENTS FOR ZERO VELOCITY EXPERIMENT

BLOCKAGE CONFIGURATION (A)

Measuring Position (Figure 7)	Axial Distance from Rear of Blockage (inches)							
	4.94	5.19	5.44	5.94	6.94	7.94	8.94	13.94
3,2	.000	.329	.492	.823	.960	1.030	.780	.743
4,2	.171	.410	.581	.850	.961	1.010	.756	.730
5,2	.129	.393	.608	1.023	.968	.987	.735	.722
6,2	.282	.463	.651	1.083	.960	.980	.724	.728
5,1	.230	.396	.582	.973	.912	.907	.672	.666
5,3	.140	.378	.590	.674	.895	.997	.724	.733

TABLE 2

NORMALIZED VELOCITY MEASUREMENTS FOR FLOW RATE RECOVERY EXPERIMENT

BLOCKAGE CONFIGURATION (A)

Subchannel	Position	Axial Distance from Rear of Blockage																
(Figure 6)	(Fig. 7)	-21.56	-16.56	-11.56	-6.56	-4.06	-1.56	9.94	14.94	19.94	24.94	29.94	34.94	39.94	44.94	49.94	54.94	59.94	64.94
2,2	7,1	1.012	1.006	.983	.935	.880	.792	.988	.932	.947	.952	.989	1.013	1.016	.997	1.001	1.005	1.027	.997
2,2	7,4	1.205	1.205	1.219	1.202	1.162	1.092	.844	.957	1.012	1.071	1.124	1.150	1.157	1.151	1.1165	1.171	1.180	1.177
2,2	2,4	1.213	1.191	1.189	1.171	1.138	1.129	1.225	1.193	1.151	1.131	1.134	1.125	1.098	1.080	1.074	1.047	1.041	1.066
2,2	5,5	1.194	1.194	1.199	1.203	1.190	1.163	.850	.983	1.040	1.107	1.150	1.165	1.167	1.170	1.173	1.176	1.187	1.190
2,2	4,7	1.144	1.139	1.132	1.116	1.108	1.129	.895	.953	1.077	1.136	1.152	1.164	1.155	1.147	1.124	1.085	1.138	1.130
2,2	Avg.	1.154	1.147	1.145	1.125	1.096	1.061	.960	1.003	1.046	1.080	1.110	1.123	1.119	1.109	1.108	1.097	1.114	1.112
2,3	7,1	1.023	.978	.977	.967	.909	.590	.610	.717	.766	.806	.824	.820	.792	.790	.807	.821	.875	.903
2,3	7,4	1.291	1.273	1.242	1.210	1.156	.924	.838	.787	.869	.881	.934	.964	.977	.982	1.001	1.014	1.044	1.075
2,3	2,4	1.077	1.069	1.075	1.066	1.024	.846	.793	.783	.828	.927	.991	1.026	1.014	1.025	1.049	1.060	1.064	1.064
2,3	5,5	1.230	1.218	1.208	1.195	1.146	.923	.729	.782	.835	.884	.942	.973	.983	1.005	1.018	1.036	1.051	1.069
2,3	4,7	1.127	1.119	1.120	1.113	1.067	.865	.865	.801	.820	.859	.904	.929	.936	.943	.944	.936	.997	1.039
2,3	Avg.	1.149	1.131	1.124	1.110	1.060	.830	.767	.774	.824	.871	.919	.943	.940	.949	.964	.978	1.006	1.030
2,4	7,1	.953	.968	.958	.949	.922	.871	.880	.953	.988	.993	1.030	1.014	.962	.942	.970	.955	.995	1.006
2,4	7,4	1.194	1.194	1.187	1.180	1.154	1.152	1.014	1.166	1.184	1.191	1.197	1.183	1.158	1.148	1.154	1.162	1.175	1.177
2,4	2,4	1.222	1.202	1.181	1.143	1.098	.998	.895	.935	.985	1.037	1.061	1.055	1.026	1.011	1.037	1.058	1.121	1.146
2,4	5,5	1.227	1.228	1.229	1.223	1.203	1.159	.997	1.119	1.157	1.180	1.193	1.180	1.163	1.157	1.148	1.165	1.169	1.175
2,4	4,7	1.152	1.167	1.158	1.192	1.132	1.080	1.278	1.202	1.172	1.185	1.181	1.176	1.144	1.132	1.124	1.131	1.142	1.136
2,4	Avg.	1.149	1.152	1.143	1.137	1.102	1.052	1.013	1.075	1.097	1.117	1.132	1.122	1.091	1.078	1.087	1.094	1.121	1.128
3,6	7,1	.955	.967	.981	.929	.916	.958	1.106	1.043	1.011	.966	.951	.923	.906	.922	.886	.896	.872	.867
3,6	7,4	1.129	1.132	1.137	1.141	1.132	1.137	1.000	1.094	1.110	1.122	1.115	1.095	1.080	1.057	1.042	1.029	1.020	1.048
3,6	2,4	1.147	1.134	1.111	1.076	1.035	1.020	1.047	1.121	1.136	1.166	1.145	1.112	1.084	1.061	1.055	1.031	.952	1.028
3,6	5,5	1.173	1.177	1.180	1.173	1.138	1.086	.880	1.058	1.097	1.109	1.102	1.070	1.082	1.063	1.065	1.048	1.041	1.057
3,6	4,7	1.149	1.145	1.112	1.085	1.024	.994	.838	.890	.918	.950	.961	.961	.985	.988	.991	.988	.989	.988
3,6	Avg.	1.111	1.111	1.104	1.081	1.049	1.039	.974	1.041	1.054	1.063	1.055	1.032	1.027	1.018	1.008	.998	.975	.998

TABLE 3

NORMALIZED VELOCITY MEASUREMENTS FOR ZERO VELOCITY EXPERIMENT

BLOCKAGE CONFIGURATION (B)

Measuring Position (Figure 7)	Axial Distance from Rear of Blockage (inches)						
	9.94	10.94	11.94	12.94	13.94	14.94	19.94
1,3	.236	0.301	.365	.413	.458	.502	.666
2,3	.000	0.0167	.286	.358	.413	.447	.625
3,3	.000	0.000	.214	.312	.377	.410	.589
5,3	.000	0.000	.194	.301	.369	.396	.573
7,3	.000	0.075	.233	.327	.365	.430	.569
8,3	.000	0.186	.296	.367	.422	.447	.592
9,3	.211	0.312	.378	.427	.470	.500	.611
5,1	.000	0.000	.987	.289	.321	.365	.510
5,2	.000	0.000	.204	.294	.363	.405	.560
5,4	.000	0.000	.175	.289	.365	.402	.571
5,5	.000	0.000	.140	.269	.346	.396	.574
5,6	.000	0.000	.099	.250	.336	.393	.575
5,7	.000	0.000	.124	.266	.352	.412	.591
5,8	.000	0.000	.186	.303	.386	.441	.615
5,9	.000	0.118	.256	.354	.427	.478	.644

TABLE 4

NORMALIZED VELOCITY MEASUREMENTS FOR FLOW RATE RECOVERY EXPERIMENT

BLOCKAGE CONFIGURATION (B)

Subchannel (Figure 6)	Position (Fig. 7)	Axial Distance from Rear of Blockage																
		-21.56	-16.56	-11.56	-6.56	-4.06	-1.56	9.94	14.94	19.94	24.94	29.94	34.94	39.94	44.94	49.94	54.94	59.94	64.94
2,2	7,1	1.010	.938	.968	.877	.731	–	.460	.539	.645	.758	.814	.849	.863	.876	.896	.891	.914	.913
2,2	7,4	1.207	1.212	1.207	1.150	1.052	.694	.513	.600	.763	.854	.925	.969	.994	1.011	1.032	1.039	1.057	1.061
2,2	2,4	1.204	1.188	1.164	1.115	1.039	.876	.743	.726	.831	.912	.958	.981	.987	.989	.990	.988	.992	1.013
2,2	5,5	1.189	1.193	1.189	1.164	1.085	.820	.519	.661	.819	.903	.958	.990	1.008	1.018	1.030	1.037	1.045	1.059
2,2	4,7	1.133	1.112	1.109	1.055	1.034	.958	.669	.775	.921	.964	1.005	1.014	1.016	1.024	1.007	1.001	1.015	1.014
2,2	Avg.	1.149	1.141	1.127	1.072	.988	.670	.581	.660	.800	.878	.931	.961	.974	.984	.991	.991	1.005	1.012
2,3	7,1	1.008	.970	.948	.885	.728	.235	.160	.396	.517	.604	.667	.713	.742	.760	.796	.810	.844	.875
2,3	7,4	1.264	1.227	1.196	1.120	.989	.666	–	.422	.567	.682	.764	.831	.875	.899	.937	.960	.987	1.020
2,3	2,4	1.058	1.073	1.055	1.001	.879	.599	–	.454	.605	.727	.815	.874	.920	.945	.973	.987	1.001	1.020
2,3	5,5	1.223	1.197	1.185	1.119	.994	.655	–	.403	.563	.683	.769	.844	.888	.915	.950	.971	.991	1.016
2,3	4,7	1.117	1.095	1.112	1.067	.957	.678	–	.396	.560	.680	.766	.825	.861	.885	.907	.928	.957	.993
2,3	Avg.	1.133	1.112	1.099	1.038	.910	.567	.028	.414	.562	.675	.756	.817	.857	.881	.913	.931	.956	.985
2,4	7,1	.948	.944	.947	.892	.766	.241	.350	.589	.671	.732	.779	.780	.800	.785	.825	.847	.871	.905
2,4	7,4	1.176	1.106	1.156	1.105	1.030	.794	.600	.657	.748	.825	.882	.916	.931	.936	.963	.981	1.005	1.029
2,4	2,4	1.153	1.143	1.118	1.042	.918	.611	.456	.525	.635	.737	.808	.860	.894	.907	.944	.969	.991	1.021
2,4	5,5	1.204	1.199	1.191	1.147	1.059	.798	.676	.626	.704	.808	.889	.924	.938	.944	.968	.985	1.007	1.019
2,4	4,7	1.167	1.165	1.141	1.102	.982	.742	.778	.679	.838	.874	.943	.954	.947	.946	.951	.967	.979	1.007
2,4	Avg.	1.130	1.111	1.111	1.058	.951	.637	.570	.615	.719	.795	.860	.887	.902	.904	.930	.950	.971	.996
3,6	7,1	.986	.989	1.006	.988	.938	.861	.835	.755	.815	.837	.876	.919	.928	.935	.936	.923	.910	.920
3,6	7,4	1.124	1.122	1.116	1.094	1.044	1.206	.743	.795	.906	.947	.977	.995	1.006	1.011	1.013	1.012	1.011	1.020
3,6	2,4	1.156	1.137	1.103	1.031	.921	.672	.614	.606	.729	.843	.906	.932	.949	.955	.976	.986	.998	1.007
3,6	5,5	1.168	1.162	1.156	1.106	.993	.753	.606	.650	.803	.876	.923	.948	.970	.979	.997	1.013	1.024	1.045
3,6	4,7	1.137	1.147	1.125	1.055	.954	.759	.346	.548	.706	.815	.853	.911	.938	.957	.983	1.003	1.018	1.037
3,6	Avg.	1.114	1.111	1.101	1.055	.970	.850	.629	.671	.792	.864	.907	.941	.958	.967	.981	.988	.992	1.006
3,1	7,1	1.105	1.079	1.062	.988	.909	1.029	1.393	1.178	1.111	1.062	1.055	1.069	1.052	1.056	1.044	1.011	.981	.967
3,1	7,4	1.217	1.203	1.198	1.195	1.167	1.169	1.133	1.250	1.231	1.198	1.173	1.151	1.131	1.099	1.095	1.095	1.099	1.114
3,1	2,4	1.155	1.138	1.125	1.053	.987	1.085	.812	1.079	1.131	1.150	1.149	1.143	1.120	1.071	1.053	1.041	1.027	1.022
3,1	5,5	1.227	1.209	1.192	1.155	1.110	1.074	.971	1.160	1.196	1.200	1.191	1.178	1.162	1.131	1.124	1.123	1.125	1.133
3,1	4,7	1.100	1.079	1.062	1.026	.967	.976	.947	1.057	1.098	1.113	1.106	1.084	1.068	1.053	1.052	1.059	1.062	1.062
3,1	Avg.	1.161	1.142	1.128	1.083	1.028	1.067	1.051	1.145	1.153	1.145	1.135	1.125	1.106	1.082	1.074	1.066	1.059	1.060
1,5	7,1	.957	.948	.948	.953	.974	1.149	1.224	1.132	1.074	1.017	.983	.969	.938	.925	.930	.931	.954	.967
1,5	7,4	1.182	1.146	1.155	1.131	1.153	1.233	1.165	1.269	1.250	1.217	1.197	1.174	1.154	1.139	1.136	1.138	1.146	1.160
1,5	2,4	1.177	1.157	1.155	1.116	1.077	.988	1.115	1.154	1.118	1.103	1.103	1.100	1.097	1.096	1.107	1.119	1.131	1.138
1,5	5,5	1.228	1.211	1.202	1.214	1.173	1.147	.966	1.168	1.212	1.222	1.212	1.187	1.169	1.152	1.154	1.158	1.169	1.181
1,5	4,7	1.281	1.251	1.223	1.103	1.027	1.065	1.027	1.119	1.159	1.217	1.178	1.176	1.166	1.151	1.153	1.153	1.157	1.144
1,5	Avg.	1.165	1.143	1.137	1.103	1.081	1.117	1.099	1.169	1.163	1.155	1.135	1.121	1.105	1.093	1.096	1.100	1.111	1.118
1,4	7,1	.951	.943	.941	.934	.926	1.000	.995	.847	.870	.882	.887	.898	.890	.890	.905	.918	.950	.965
1,4	7,4	1.147	1.152	1.135	1.088	1.037	1.022	.977	.988	1.010	1.037	1.062	1.087	1.107	1.113	1.131	1.149	1.178	1.183
1,4	2,4	1.141	1.155	1.130	1.122	1.145	1.217	.902	.995	1.139	1.175	1.176	1.176	1.170	1.163	1.163	1.178	1.179	1.168
1,4	5,5	1.159	1.159	1.167	1.145	1.100	1.031	.883	1.020	1.021	1.049	1.094	1.125	1.143	1.154	1.170	1.185	1.201	1.209
1,4	4,7	1.132	1.146	1.153	1.111	1.077	1.099	1.206	1.157	1.066	1.045	1.061	1.092	1.105	1.112	1.116	1.122	1.126	1.129
1,4	Avg.	1.106	1.111	1.105	1.080	1.057	1.074	.993	1.001	1.021	1.037	1.056	1.076	1.083	1.086	1.097	1.110	1.127	1.131

CONF-750804--9

Westinghouse Research Laboratories

Measurements of Velocities Downstream of Blocked Subchannels in a Model Reactor Rod Bundle.

Conference Paper

R.A. Markley
B.J. Vegter

ASME

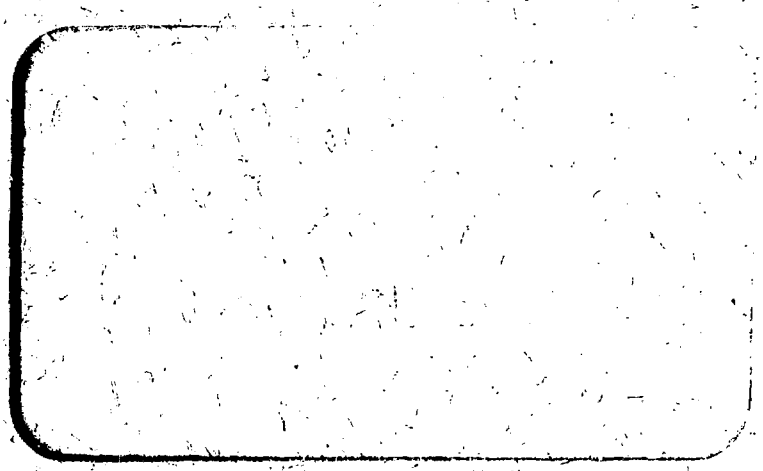

MASTER

Fran., Cal 8/11-13/75

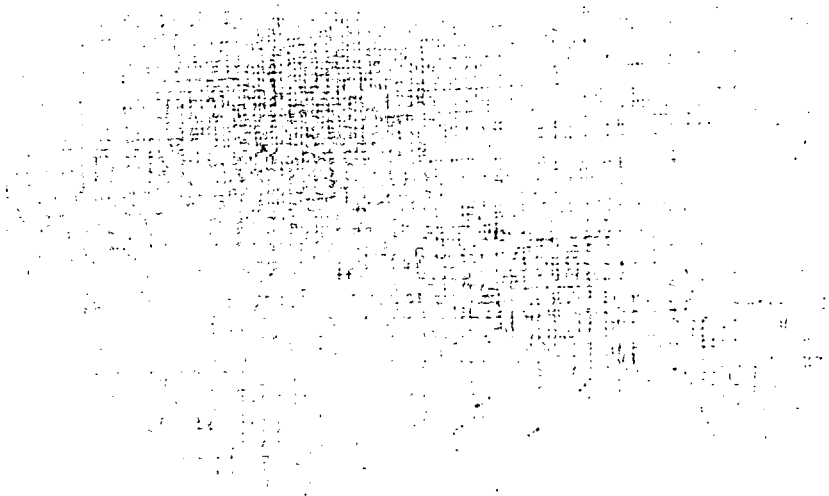

Westinghouse Research Laboratories
TECHNICAL DOCUMENT SUMMARY

UNRESTRICTED

Daniel Berg 12-30-74
Director Date

Document No.: 74-8E9-RODS-R1 Proprietary Class: Unrestricted Date: December 30, 1974

Title: MEASUREMENTS OF VELOCITIES DOWNSTREAM OF BLOCKED SUBCHANNELS IN A MODEL REACTOR ROD BUNDLE

Author(s): B.J. Vegter and R.M. Roidt
M.J. Pechersky and R.A. Markley

Department: Heat Transfer and Fluid Dynamics
Advanced Reactors Division

Pages: 35 References: 3

Keywords: LMFBR, blockage, grids, reactors, flow, cores/reactors, velocity, recovery, subchannel

ABSTRACT:

Two blockage configurations were installed on the upstream end of a hexagonal grid in an 11:1 scale 39 rod bundle air model of a liquid metal fast breeder reactor. Velocities were measured in subchannels behind and adjoining the blockages. The region of separated flow were found to be five times a characteristic height of the blockages, consistent with other experimental results. The effect of the grids on the length of separated flow was minimal. Flow rates in subchannels centered downstream of the blockages recovered to 90% of the upstream flow rates in the 28 rod diameter length between grids.

SUMMARY (Purpose, Sponsor, Approach, Conclusions, Significance):

One proposed design of a LMFBR employs hexagonal grids for supporting fuel rods. In such a design the most likely accidental blockage would occur from the collection of debris suspended in the fluid at the upstream end of the grid. This investigation examined the length of the separated flow region and the recovery of subchannel flow rate with distance downstream for two blockage configurations.

TO RESEARCH LABORATORIES LIBRARY

SEND COPY OF DOCUMENT NO. 74-8E9-RODS-R1 TO:

☐ Hard Copy* ☐ Microfiche

Name _____

Plant _____

Dept. _____

Charge No. _____

(Print plainly, this is your mailing label)

*No charge until out of stock. Then, hard copy will be furnished only when you request it and include your complete charge number to cover the $0.25/page charge and a $1.00 service charge. Otherwise, once hard copies are gone microfiche copies will be furnished routinely, at no cost.

RM-57870